ECS Transactions, 103 (1) 2163-2172 (2021)
10.1149/10301.2163ecst ©The Electrochemical Society

Electrical Conductivity of $La_{0.9}Sr_{0.1}Ga_{0.8}Mg_{0.2}O_{3-y}$-$La_{1.55}Sr_{0.45}Ga_3O_{7+\delta}$ Composite Electrolyte

T. G. Fujimoto[a,b], M. C. Steil[b], and E. N. S. Muccillo[a]

[a]Energy and Nuclear Research Institute - IPEN, PO Box 11049, S.P., 05422-970, Brazil
[b]Univ. Grenoble Alpes, CNRS, Grenoble INP, LEPMI, 38000 Grenoble, France

Doped lanthanum gallate constitutes a family of solid electrolytes with high ionic conductivity, wide electrolytic domain and good chemical stability. The combination of its properties turns some compounds of this family promising candidates for application in solid oxide cells operating at intermediate temperatures. In this work, $La_{0.9}Sr_{0.1}Ga_{0.8}Mg_{0.2}O_{3-y}$ - $xLa_{1.55}Sr_{0.45}Ga_3O_{7+\delta}$ with x = 0, 1 and 5 wt.% were investigated aiming to obtain a composite solid electrolyte with optimized properties compared to the parent material. Composite electrolytes were prepared by solid state reaction method and evaluated for densification, phase content and microstructure. Electrical conductivity measurements were carried out as a function of temperature and oxygen partial pressure. Increase on densification and structural homogeneity were obtained with increasing fraction of the melilite phase. The electrical conductivity determined by impedance spectroscopy revealed a decrease of the bulk resistivity for increasing amounts of $La_{1.55}Sr_{0.45}Ga_3O_{7+\delta}$.

Introduction

Composite materials are thoroughly used in electrochemical devices such as Solid Oxide Cells (SOCs), especially as anodes and cathodes. In general, these composite ceramics have shown better performance accounting for improvements on several properties like decrease of the area specific resistance, reduction of carbon contamination and increase of the electrical conductivity (1-3). Less investigated is the exploitation of composite solid electrolytes for application in SOCs.

Lanthanum gallate doped with partial substitutions for strontium and magnesium, with attributes such as higher ionic conductivity than yttria-stabilized zirconia, transference number equal to 1 over a wide oxygen partial pressure range and good compatibility with other cell components, is a candidate for application in SOCs operating at intermediate temperatures (~ 500 to 700 °C) (4). The typical crystalline structure of doped lanthanum gallate is related to the concentration of strontium and magnesium. In addition, impurity phases are usually detected even in chemically synthesized powders (5, 6). In general, the contents of impurity phases are low ($\leq$ 5%) turning its influence negligible in as-prepared ceramics (7). Nevertheless, their influence on long-term operation is still a subject of concern.

The compound $La_{0.9}Sr_{0.1}Ga_{0.8}Mg_{0.2}O_{3-y}$, hereafter LSGM, exhibits orthorhombic structure, good ionic conductivity and relatively low fraction of impurity phases (8). The composite electrolyte consisting of $Ce_{0.85}Sm_{0.15}O_{1.925}$- $La_{0.9}Sr_{0.1}Ga_{0.8}Mg_{0.2}O_{3-y}$, SDC-LSGM, in the 9:1 proportion, was reported to display superior conductivity than pure SDC (9). Addition of LSGM to SDC was also found to enlarge the electrolytic domain of SDC (10). Similar effects were found for $La_{0.8}Sr_{0.2}Ga_{0.8}Mg_{0.2}O_{3-\delta}$ -$Ce_{0.9}Gd_{0.1}O_{1.95}$ composites (11). Recently, composites containing $La_{0.9}Sr_{0.1}Ga_{0.8}Mg_{0.2}O_{3-y}$ - 8YSZ, as minor phase (up to 20 wt.%) were shown to exhibit better phase stability than the major phase (LSGM). Particularly, for composites containing 10 wt.% 8YSZ reduction of impurity phase contents were found (12).

In this work, the effects of small amounts of strontium-doped lanthanum gallate, LSG, with melilite structure to LSGM was studied. The main purpose of this work was to examine the effects of LSG on phase purity and ionic conductivity of LSGM.

Experimental

The compound $La_{0.9}Sr_{0.1}Ga_{0.8}Mg_{0.2}O_{3-y}$ was prepared by solid state reaction method as described in (13). The starting materials La_2O_3 (99.9%), $SrCO_3$ (99.99%), Ga_2O_3 (99.99%) and MgO (P.A.) were used as-received without further purification. The $La_{1.55}Sr_{0.45}Ga_3O_{7+\delta}$ nominal compound was synthesized by the solid state reaction method. In this case, strontium and gallium starting materials were dried at 300 °C for 3 h, and the lanthanum precursor was heat treated at 1000 °C for 3 h. Afterwards, stoichiometric amounts of the dried precursors were weighted, mixed together in alcoholic medium, dried in an oven at 40 °C and calcined at 1250 °C for 4 h.

Composite electrolytes containing x wt.% LSG, with x = 0, 1 and 5 were prepared by mixing the required amounts of LSGM and LSG, followed by pressing into discs (ϕ 9 mm and thickness ~3 mm) with 50 MPa of applied pressure. Sintering was performed at 1450 °C in air.

Phase analysis was conducted by X-ray diffraction, XRD (Bruker-AXS, D8 Advance) in the $20 \leq 2\theta \leq 80°$ range. Sintered density values were determined by the water immersion method. Microstructure characterization was performed by field emission gun scanning electron microscopy, FEG-SEM (FEI, Inspect F50) on polished and thermally etched surfaces of selected specimens. The mean grain size of sintered specimens was estimated by the intercept method.

The electrical conductivity was determined by electrochemical impedance spectroscopy. Impedance spectroscopy, IS, measurements were carried out at ambient pressure (pO_2=0.21 atm) with a LF impedance analyzer (HP, 4192A) under 200 mV of applied AC signal in the 250-550 °C range. Silver paste was applied onto large surfaces of specimens and cured at 400 °C before measurements. The recorded impedance spectra were deconvoluted by special software (14).

IS measurements were also carried out as a function of the oxygen partial pressure from 1 to 10^{-24} atm at 700, 800 and 900 °C. Several gases were utilized in this case (synthetic air, Ar, O_2 and H_2) with 4 $L.h^{-1}$ flow rate. Platinum was used as electrode material after firing

at 1100 °C. Data were collected in a Solartron SI 1260 and analyzed using ZView software.

Results and Discussion

Figure 1 shows the XRD patterns of the prepared LSG powder and of the PDF 45-637 file of the melilite phase. The experimental diffraction pattern reveals that pure tetragonal and single-phase material was obtained. No impurity neither secondary phases were detected.

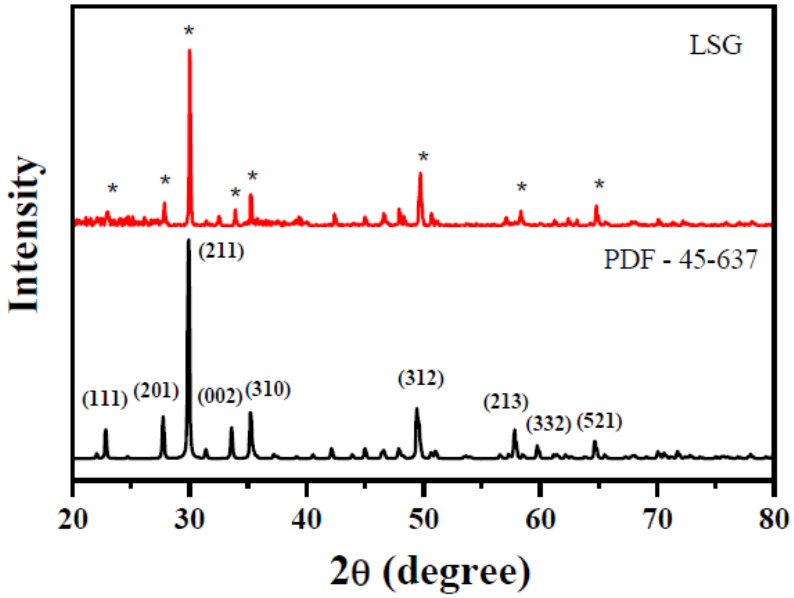

Figure 1. XRD patterns of the prepared LSG powder and of the PDF file of the melilite structure.

The XRD patterns of pure LSGM and LSGM-LSG composites containing 1 and 5 wt.% are depicted in Figure 2. The pattern of the PDF 51-290 file of the orthorhombic phase of LSGM is also shown for comparison. The XRD patterns in the left-side correspond to the whole angular range, whereas those in the right-side highlight the 2θ between 24 and 32°, where the high-intensity peaks of impurity phases in LSGM are usually found.

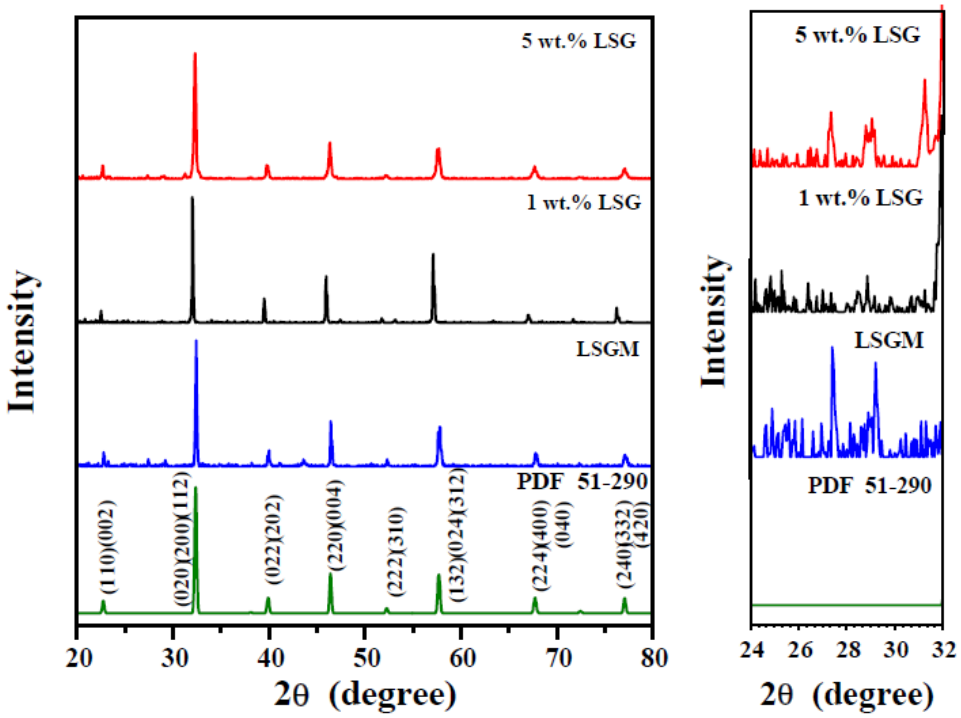

Figure 2. XRD patterns of pure LSGM and LSGM-LSG composites in the (left) 20-80° and (right) 24-32° angular ranges.

The XRD pattern of pure LSGM shows the characteristic reflections of the orthorhombic structure along with low-intensity peaks of the $La_4Ga_2O_9$ (2θ ~27°) and $LaSrGa_3O_7$ (2θ ~30°), easily identified in the right-side pattern. Composites of LSGM-LSG exhibit similar XRD reflections of the major phase (LSGM). Nevertheless, a careful examination of the small-angle region (right-side) reveals that the fraction of impurity phases becomes negligible for 1 wt.% addition of LSG to LSGM.

The relative density of sintered LSGM is 98.3% and achieved 99.7% in composites with 5 wt.% LSG suggesting a beneficial effect of the minor phase on densification of LSGM.

The FEG-SEM micrographs of polished and thermally etched surfaces of sintered specimens are shown in Figure 3. The main microstructure features are polygonal grains with both smooth and rough surfaces, besides negligible porosity. The mean grain size of sintered specimens is in the 5.5-6.7 μm range. The different texture of grains in LSGM was already reported and attributed to several factors, such as stacking faults and changes in the microstructure due to thermal stress occurring during cooling down from the high sintering temperature (15,16).

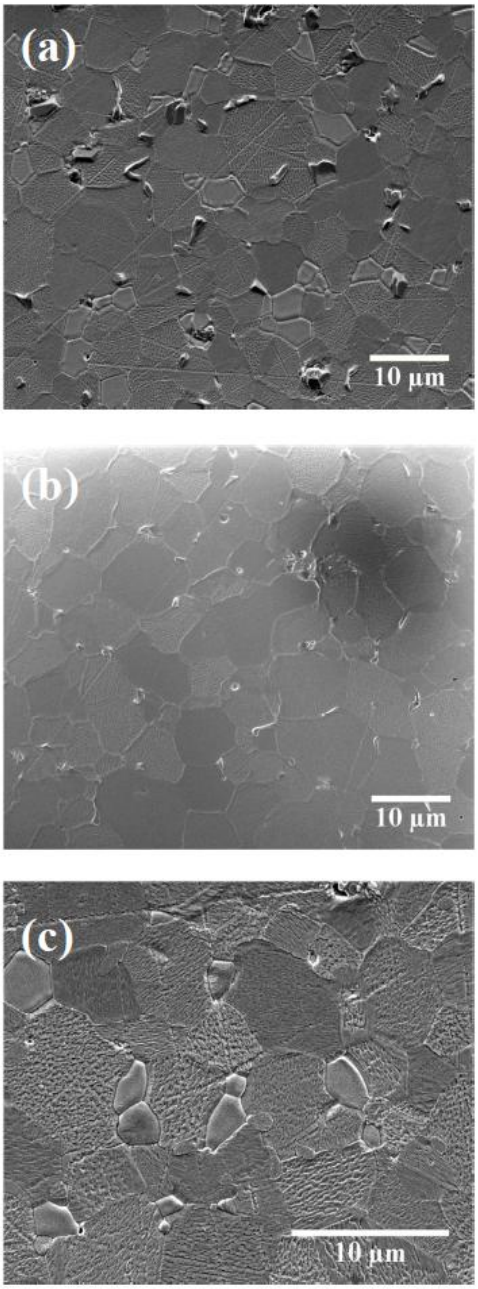

Figure 3. FEG-SEM micrographs of sintered composites of (a) pure LSGM, and (b) and (c) LSGM containing 1 and 5 wt.% LSG, respectively.

IS diagrams of pure LSGM and LSGM-LSG composites are shown in Figure 4. In these diagrams the numbers are the relaxation frequency (in Hz), and the real (Z') and imaginary (-Z'') components of total impedance were normalized for specimen dimensions. These IS spectra were measured at 275 °C in pO_2=0.21 atm.

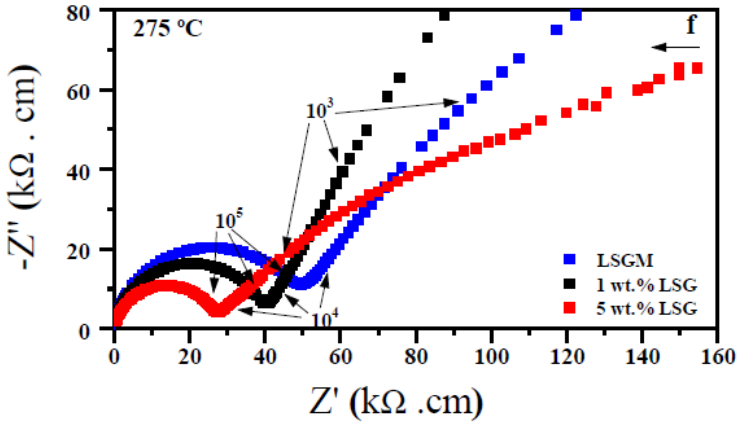

Figure 4. IS spectra of pure LSGM and LSGM-LSG composites at 275 °C.

All IS diagrams recorded in the temperature range of measurements show the same characteristics: a well-resolved high frequency arc due to the bulk resistivity and a strong overlapping between the low-intensity grain boundary (intermediate frequency) and the electrode arcs (low frequency). Then, only the bulk conductivity could be resolved in these diagrams. The electrode arc in these diagrams assures the ionic character of the conductivity over the temperature range of measurements.

Figure 5 shows the temperature dependence of the ionic conductivity of pure LSGM and LSGM-LSG composites. Surprisingly, the bulk conductivity of composites is higher than that of pure LSGM. It is known that ionic conductivity of La-rich compounds in the $La_{1+x}Sr_{1-x}Ga_3O_{7+z}$, ($x \geq 1$), is close but lower than that of LSGM (17).

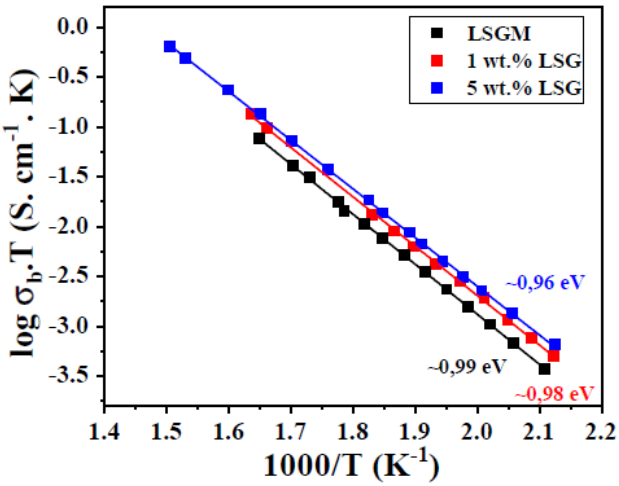

Figure 5. Temperature dependence of the ionic conductivity of pure LSGM and LSGM-LSG composites.

The activation energy values indicated in Figure 5 are of the same order of magnitude and within experimental errors, but clearly show a tendency to decrease with increasing the fraction of LSG in the composites.

Initial studies on the melilite phase indicated that the total conductivity may be tuned by varying the La:Sr ratio with La-rich compounds exhibiting total conductivity values in the same range of pure LSGM (18). Subsequently, the conductivity dependence on the oxygen partial pressure, in the 700-900 °C range, was determined and the results pointed to a p-type behavior (17). Further investigation of La-rich melilite phase (with x=1.64) evidenced a wide electrolytic domain (from 1 to ~10^{-22} atm) at 600 °C (19). Then, the behavior of LSGM-LSG composites was worth to be investigated.

Figure 6 depicts the evolution of the bulk conductivity of (a) LSGM and composites of (b) LSGM + 1 wt.% LSG and (c) LSGM + 5 wt.% LSG as a function of the oxygen partial pressure.

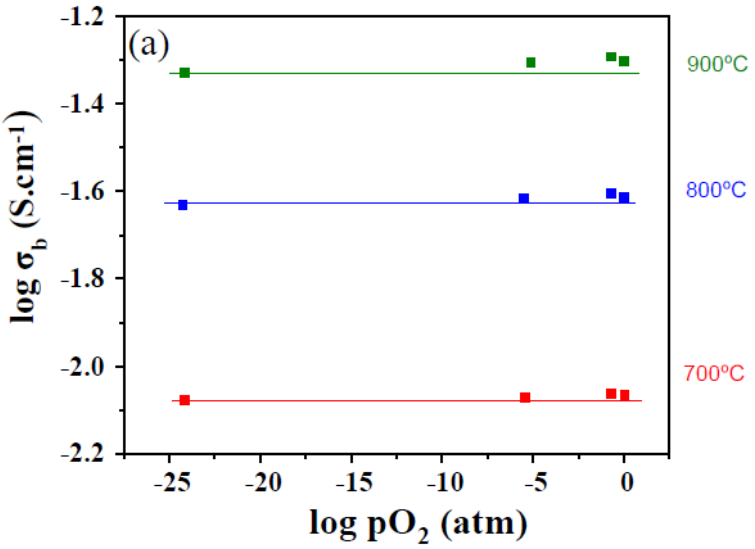

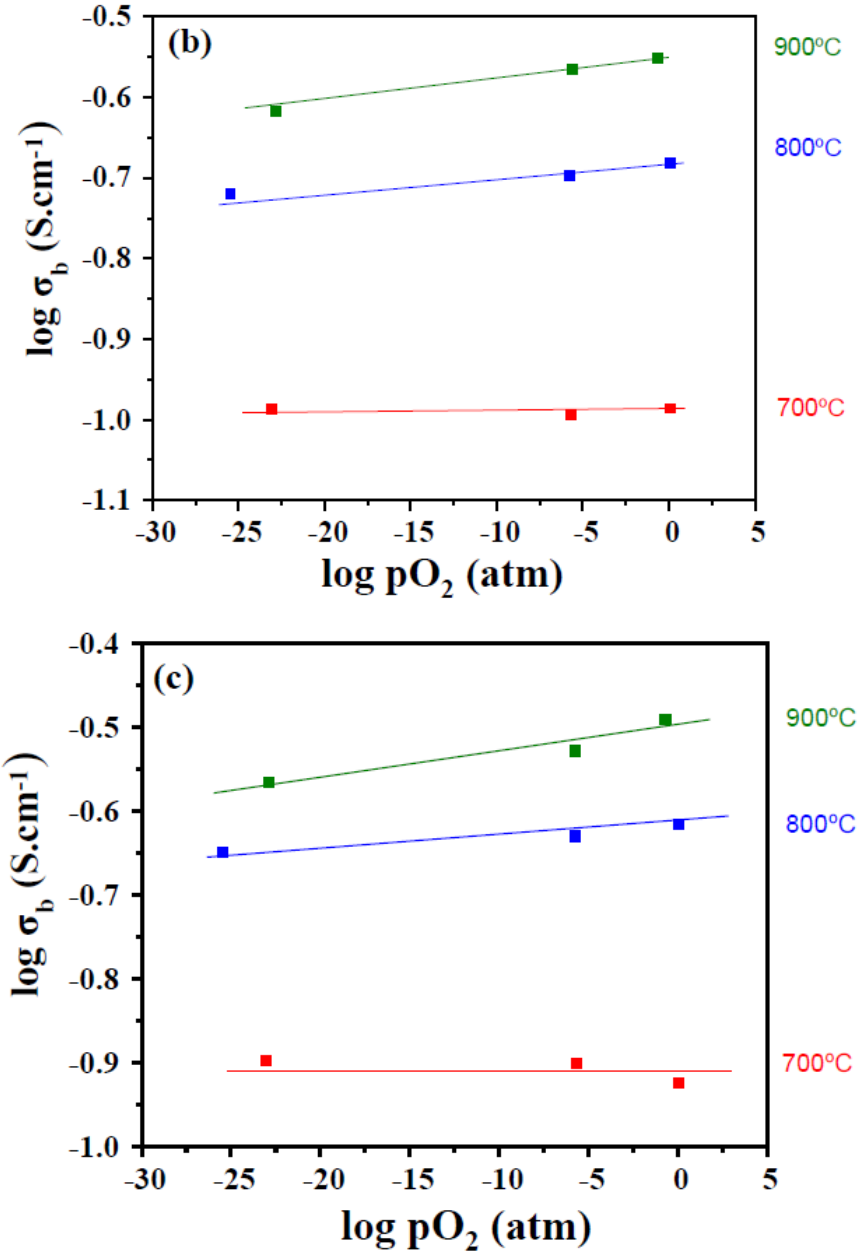

Figure 6. Temperature dependence of the ionic conductivity of pure LSGM and LSGM-LSG composites.

The bulk conductivity of pure LSGM (Figure 6a) is constant with the oxygen partial pressure in the 700-900 °C range, as expected. The composites (Figure 6b and 6c) also exhibit wide electrolytic domain at 700 °C. Nevertheless, at higher temperatures, the positive slope of the fitting lines suggests non negligible electronic p-type conduction, thereby establishing a limit for application of LSGM-LSG composites in SOCs.

Conclusions

Composite solid electrolytes consisting of $La_{0.9}Sr_{0.1}Ga_{0.8}Mg_{0.2}O_{3-y}$-x$La_{1.55}Sr_{0.45}Ga_3O_{7+z}$ (LSGM-xLSG) were prepared by the solid state reaction method. The sintered materials achieved high relative densities (> 98%) after sintering at 1450 ºC. Addition of only 1 wt.% LSG was efficient to minimize the fraction of impurity phases of LSGM. The microstructure of composites is similar to that of the parent electrolyte with negligible porosity and mean grain size in the 5.5 to 6.7 μm range. The electrical conductivity of composites was found purely ionic up to 700 ºC, allowing their application in SOCs operating at intermediate temperatures. In the low temperature range, the ionic conductivity of composites is slightly higher than that of pure LSGM, with activation energy values of approximately 0.98 eV.

Acknowledgments

The authors acknowledge FAPESP (2013/07296-2 and 2017/11937-4), CNPq (305889/2018-4) and CAPES (88887.371190/2019-00) for financial supports.

References

1. L. H. Lu, Q. L. Shi, Y. Yang and H. Zhang, *Mater. Res. Bull.*, **47**, 1010 (2012).
2. B. Huang, X. J. Zhu, W. Q. Hu, Y. Y. Wang and Q. C. Yu, *J. Power Sources,* **195**, 3053 (2010).
3. F. C. Fonseca, D. Z. de Florio, V. Esposito, E. Traversa, E. N. S. Muccillo and R. Muccillo, *J. Electrochem. Soc.*, **153**, A354 (2006).
4. T. Ishihara, H. Matsuda and Y. Takita,*J. Am. Chem. Soc.*, **116**, 3801 (1994).
5. K. Huang and J. B. Goodenough, *J. Solid State Chem.*, **136**, 274 (1998).
6. S. L. Reis and E. N. S. Muccillo, *Adv. Mater. Res.*,**975**,81 (2014).
7. D. Marrero-López, J. C. Ruiz-Morales, J. Peña-Martinez, M. C. Martin-Sedeño, and J. R. Ramos-Barrado, *Solid State Ionics,***186**, 44 (2011).
8. P. N. Huang and A. Petric, *J. Electrochem. Soc.*, **143**, 1644 (1996).
9. D. Xu, X. Liu, D. Wang, G. Yi, Y. Gao, D. Zhang, and W. Su, *J. Alloy. Compd.*, **429**, 292 (2007).
10. G. Hao, X. Liu, H. Wang, H. Be, L. Pei, and W. Su, *Solid State Ionics,***225**, 81 (2012).
11. S. H. Jo, P. Muralidharan, and D. K. Kim,*J. Alloy. Compd.*, **491**, 416 (2010).
12. T. G. Fujimoto, S. L. Reis, and E. N. S. Muccillo,*Mater. Res.*, **22**(S1), e20190043 (2019).
13. S. L. Reis, E. N. S. Muccillo, *Ionics*, **24**, 1693 (2018).
14. M. Kleitz and J. H. Kennedy,in *Fast Ion Transport in Solids, Electrodes and Electrolytes*, P. Vashishta, J. N. Mundy, and G. K. Shenoy, Editors, p. 1858, North-Holland, Amsterdam, (1979).
15. X. Zao, X. Li, N. Xu, and K. Huang,*Solid State Ionics,***214**, 56 (2012).
16. Y.-C. Wu and M.-Z. Lee,*Ceram. Int.,***39**, 56 (2013).
17. M. Rozumek, P. Majewski, H. Schluckwerder, F. Aldinger, K. Künstler, and G. Tomandl, *J. Am. Ceram. Soc.,***87**, 1795 (2004).

18. M. Rozumek, P. Majewski, F. Aldinger, K. Künstler, and G. Tomandl,*Ber. DKG,* **80**, E35 (2003).
19. Thomas. C. I. Thomas, X. Kuang, Z. Deng, H. Niu, J. B. Claridge, and M. J. Rosseinsky, *Chem. Mater.,***22**, 2510 (2010).